Graduate Theses and Dissertations

2017

Measuring system value in the Ares 1 rocket using an uncertainty-based coupling analysis approach

Christopher Wenger
Iowa State University

Follow this and additional works at: https://lib.dr.iastate.edu/etd

Part of the Aerospace Engineering Commons

Measuring system value in the Ares 1 rocket using an uncertainty-based coupling analysis approach

by

Christopher Wenger

A thesis submitted to the graduate faculty

in partial fulfillment of the requirements for the degree of

MASTER OF SCIENCE

Major: Aerospace Engineering

Program of Study Committee:
Christina Bloebaum, Major Professor
Ran Dai
Peng Wei

The student author, whose presentation of the scholarship herein was approved by the program of study committee, is solely responsible for the content of this thesis. The Graduate College will ensure this thesis is globally accessible and will not permit alterations after a degree is conferred.

Iowa State University

Ames, Iowa

2017

TABLE OF CONTENTS

iv

LIST OF FIGURES

v

LIST OF TABLES

NOMENCLATURE

LSCES	Large Scale Complex Engineered Systems
MDO	Multidisciplinary Design Optimization
NASA	National Aeronautics and Space Administration
T/O	Thrust Oscillation
SRM	Solid Rocket Motor
VBD	Value Driven Design
DSM	Design Structure Matrix
RSRM	Reusable Solid Rocket Motor
CFD	Computational Fluid Dynamics
ISS	International Space Station
USD	United States Dollar

ACKNOWLEDGMENTS

I would like to start off by expressing my sincerest gratitude to my major professor and advisor, Dr. Christina Bloebaum for her support and guidance through my Masters of Science degree at Iowa State University. Her valuable advice and tolerance to my mistakes helped me grow both academically and individually. I am also very grateful that we were able to continue the research while away from campus. I would also like to thank my collegues in MODEL for there support through my studies and multiple late nights in the lab. I am truly grateful to everyone I have work with on this project, this journey will be a memorbaly one.

ABSTRACT

Coupling of physics in large-scale complex engineering systems must be correctly accounted for during the systems engineering process to ensure no unanticipated behaviors or unintended consequences arise in the system during operation. Structural vibration of large segmented solid rocket motors, known as thrust oscillation, is a well-documented problem that can affect the health and safety of any crew onboard. Within the Ares 1 rocket, larger than anticipated vibrations were recorded during late stage flight that propagated from the engine chamber to the Orion crew module. Upon investigation engineers found the root cause to be the structure of the rockets feedback onto fluid flow within the engine. The goal of this paper is to showcase a coupling strength analysis from the field of Multidisciplinary Design Optimization to identify the major impacts that caused the Thrust Oscillation event in the Ares 1. Once identified an uncertainty analysis of the coupled system using an uncertainty based optimization technique is used to identify the likelihood of occurrence for these strong or weak interactions to take place.

CHAPTER 1

INTRODUCTION

During the operational lifecycle, engineering systems may have unanticipated behaviors or unintended consequences affecting the outcome of its objective. Depending of the scale of the system the number of unexpected behaviors or consequences may increase as the systems increases in complexity. Typically, with Large Scale Complex Engineered Systems (LSCES), (i.e. Space Launch Systems, Joint Strike Fighter, Aircraft Carriers), these number of unexpected behaviors increase due to their complexity and the large amount of interactions between the systems lower level subsystems. The development of LSCES is highly demanding on time and resources, typically one system takes nearly a decade to finish and may have multiple budget overruns. If an unexpected behavior occurs during testing, methods are put into place to fix the behavior and ensuring that the system is operating as intended. Adding these fixes adds time and cost towards the program and may delay the release of the LSCES. However, if the behaviors of the system are identified and captured properly during the design and development phase, the probability of resource overrun decreases. Instead of fixing unknown issues that occur during the operational lifecycle of the system, capturing the system behaviors allows the designer to find the root causes and can prevent multiple unintended behaviors before testing. [1]

The intent of this research is to replicate the Ares 1 rocket, identify all known design characteristics and system behaviors, and perform an analysis on the system using the coupling strength approach from the field of Multidisciplinary Design Optimization (MDO)

[13]. By using this approach unintended behaviors can be identified and addressed before reaching the testing phase. In addition, uncertainty is used to identify the probability of the unintended behaviors affecting the value of the Ares 1 by understanding how each subsystem interaction changes with respect to new design inputs. The primary focus is to understand a specific phenomenon that occurred during the operation of the Ares 1-X, a prototype to the Ares 1, and analyzing how this phenomenon affects the value of the Ares 1.

The Ares 1 is a launch vehicle design part of the constellation program, intended to use the Ares 1 to launch the Orion, a crew module, into orbit for missions to the International Space Station (ISS) and later a manned mission to Mars. [2] During a test launch of the Ares 1-X large vibrations and perturbations were recorded within the engine chamber of the first stage rocket. These vibrations propagated from the first stage rocket to the crew module presenting possible hazardous operating conditions for the crew onboard the Orion. After the test launch NASA ran an investigation which pointed to Thrust Oscillation (T/O) as being the major contributing factor toward the vibrations and perturbations recorded.

Thrust oscillation is a well-known phenomenon caused by combustion instabilities within the combustion chamber of a Solid Rocket Motor (SRM). During combustion, turbulent flow is produced from geometric changes inside the combustions chamber, typically caused by a change in wall sizing or any bluff objects protruding into the flow [3]. Downstream of the bluff object vortex shedding occurs causing vortices to separate and interact with the propellant flow and surface of the engine chamber. This interaction creates a cause a surge which increases the pressure inside the combustion chamber and exerting a force along the surface of the chamber. If the vortex shedding procedures a frequency

corresponding to the acoustic modes of the rocket, the pressure is oscillating and increases the energy inside the combustion chamber. This oscillation may travel upstream and interact with the flow and increasing the instability rate [4]. The rocket's structure will interact with the energy created by the turbulent flow, if the structure's natural response is close to the vortex shedding frequency the excitation of energy generated by pressure oscillation will not dampen out [3]. If not dampened out pressure oscillation will increase in magnitude and therefore thrust oscillation will increase, causing an increase in instability in the propellant flow, and increase in vibrational forces interacting with the structure. If T/O is not mitigated, the flow inside the engine chamber may be highly instable, affecting the rocket structure, and eventually propagating up to the crew module as was in the case with the Ares 1-X [2].

Engineers at NASA conducted numerous investigations, and formed a T/O mitigation team to tackle the T/O phenomena recorded on the Ares 1-X. Multiple mitigation methods were investigate and proposed, but ultimately two additions were implemented to mitigate T/O [5]. The first method to mitigate T/O was placing C-spring isolators between the segments of the rocket, acting as a shock absorber to dampen out some of the energy created by T\O. The second method is using a LOX damper to leverage the kinetic energy of the liquid oxygen tank to dampen out the vibrations caused by the propellant flow. With the addition of the C-spring and LOX damper, the T/O team had a higher confidence factor in mitigating the T\O forces that were recorded during the Ares 1-X test launch [5].

Typically, the modeling and design for LSCES is decomposed into its subsystems and designated to teams to work on. In many cases these subsystems are distributed between different organizations and discomposed more and components are assigned to design teams.

This can cause problems in the long run, mainly when the development phase begins to integrate all the subsystem. In the case of the Ares 1 the subsystems such as fluids and structures were distributed to teams and their form of communication was using interface control documentation. Here the effects of direct inputs on one subsystem to another is captured. The initial analysis of the system showed an inconsequential feedback from structures onto fluids and was ignored to save on computational/analysis time. However, the T/O mitigation team found that the structure of the rocket does interact with the fluids inside the rocket chamber and that T/O has a higher impact than earlier predications showed. If a means existed to identifying the importance of the coupling and feedbacks in the system physics during the design phase, maybe modifications to the design could have prevented the T/O event.

In this research, an investigation of the T/O event that occurred on the Ares 1-X will be made to understand how uncertainty in each of the subsystem interactions can effect each other and the overall value of the system. This thesis proposes using a Multidisciplinary Coupling Analysis with the addition of uncertainty generated by taking multiple samples of certain design variables within the design space. This analysis will aid in understanding how the T/O event is effect by each design variable and how a change in the design effects each coupling strength propagating that change to the value model. This investigation will focus on the key contributors to the T/O event and the design space in isolated around the extrema of the T/O event which is around the 1L acoustic mode. The value model will be used to determine the impact each coupling has on the overall system value of the Ares 1.

CHAPTER 2

RESEARCH QUESTIONS

This chapter contains the research questions this thesis aims to answer and were formed by an unforeseen behavior found in the Thrust Oscillation event of the Ares 1 and how it impacted NASA and congressional support.

Research Question 1

"Can Monte Carlo Simulations be used to predict the magnitude of each coupling due to the uncertainty of design and behavior variables and predict the overall system value?"

Research Question 2

"Can a lower fidelity model be developed to simulation the Thrust Oscillation event that occurred on the Ares 1 with a reduction in computation time but maintaining accurate results?"

Research Question 3

"How can government influences impact the overall value of our system and any future programs?"

Organization of Thesis

The thesis is broken down by stating the research questions this paper aims to answer with the proposed approach to address them. Next, a detailed background of the physics associated with the Thrust Oscillation event will be covered as well as each of the disiplines that drive this event this was the major unforeseen behavior in the Ares 1, as well as the proposed methodology model Thrust Oscillation and use the model to find any uncertainty.

CHAPTER 3

BACKGROUND

Thrust Oscillation

During combustion, a sudden transitional change occurs within the SRM's chamber causing unstable shear layers, turbulent flow, and more specifically vortex shedding [4]. These vortices created by vortex shedding begin to develop after the flow has interacted with a bluff body. Once created the vortices travel downstream interacting with the SRMs nozzle causing pressure waves, known as pressure oscillation, to propagate upstream through the SRM's chamber [5]. Causing an increase of energy within the SRM's cavity this energy is translated into a force interacting with the chamber walls. Typically, the excited energy created by pressure oscillation is dampened out, causing no harm or instability to the SRM. However, in some cases pressure oscillation due to vortex shedding has a greater excitation in energy, which causes a greater structural response, known as T/O. Not mitigated properly, T/O causes unstable vibrations within the SRM's chamber propagating through the rocket, affecting both the crew on-board and the structural supports. The T/O phenomenon is linked to coupling interactions between the acoustic modes, fluid flow, and structural mode responses [4]. Ideally, the SRM's natural resonance should be a prescribed distance apart from pressure oscillation frequencies to avoid a major T/O event [1].
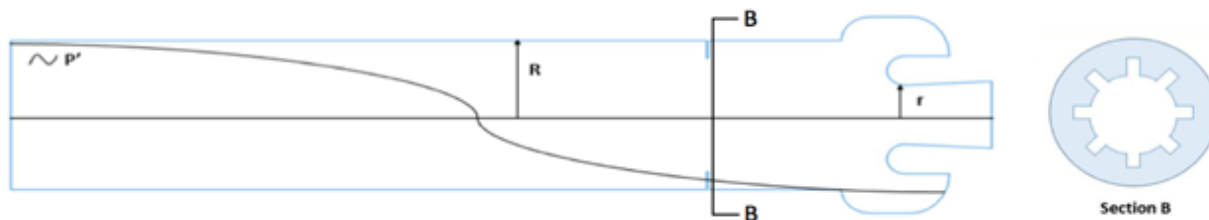
Figure 1: Diagram of solid rocket motor with inhibitor cross-section

Ares 1 Subsystem Physics

SRMs have multiple subsystems interacting with one another to complete the system's intended design objective. While there are many disciplines that interact in a SRM system analysis, this paper focuses on three key subsystems that have been previously identified to be the underlying drivers of T/O. The five main subsystems investigated in this paper are propulsion, damping systems, acoustics, fluids dynamics, and structures. How these are coupled is discussed later in this paper. In this section, we will provide an overview of the physics associated with each that drive the T/O event.

Solid-propellant rockets can be broadly classified as one of two types, either end burning or erosive burning. End burning only burns at the end, the sidewall propellant is inhibited to prevent the flame front from traveling into the propellant along the sidewall. In an erosive-burning rocket, the grain is inhibited on the end and the propellant burns in a direction perpendicular to the gas glow. Erosive-burn rockets are higher thrust, shorter duration rockets because the large burning area leads to large mass flow rate. In the example,

an erosive-burn rocket is considered for the coupling strength analysis. Here, the propellant grain size is assumed to be a 'star grain' keeping the burn rate constant as time passes. [6]
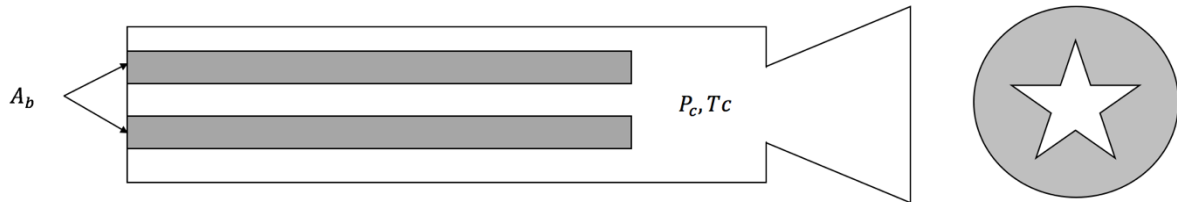
Figure 2: Diagram of solid rocket propellant with cross-section

Acoustics is a subsystem that monitors the interactions of acoustics waves within a medium. Typically, these waves are created within a duct or in our cause the combustion chamber of the SRM. As the fluid propagates through the chamber, the sound produces changes with respect to any geometry changes and changes in the fluid's velocity. With the case of SRMs, three types of acoustic waves occur in the combustion chamber: longitudinal, tangential and radial acoustic modes [7]. These modes are shown in Figure. For this study, the longitudinal mode and its interaction with pressure oscillation is the key point of interest.
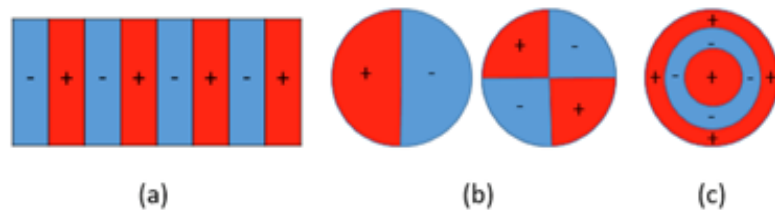
Figure 3: Diagram of solid rocket motor with inhibitor cross-section

In the fluids subsystem, pressure oscillations are generated from turbulent flow within a rocket engine (e.g. from vortex shedding). There are three types of vortex shedding that can

occur within an SRM: obstacle vortex shedding; surface vortex-shedding; and parietal vortex-shedding [8]. This paper will focus on obstacle vortex shedding as this was the major contributor to the T/O event on the Ares 1. Shearing layers that form around any blunt object that protrudes into the flow, the inhibitors in this case, generate obstacle vortex shedding. When these shear layers' form, low-pressure vortices detach and flow downstream causing pressure oscillations [5].

Once pressure oscillations are generated within the rocket chamber, the structure then responds to these cyclical loads by dampening out the excited energy in the system. The effectiveness for a structure to dampen out these cyclical loads is mostly determined by its geometry and material properties. If dampening overcomes the forces exerted onto it by pressure oscillation, the system will return to its stable state. However, in the instance of the Ares 1, excitation was larger than the dampening, leading to structural resonance of the system. These vibrations within the engine were not sufficiently dampened and propagated throughout the system, eventually affecting the crew module sufficiently as to impact potential health and function of the crew.

<div align="center">Systems Engineering</div>

Large-Scale Complex Engineered Systems are complex, multidisciplinary, and involve multiple organizations to develop. To tackle complexity of designing and certifying these types of systems, systems engineering was introduced in the 1950s. Over time development of LSCES has grown in both time and cost at unsustainable rates compared to other engineering systems, the cost is too high and the program gets discontinued [7]. Currently, systems are being designed using requirements-driven Systems Engineering (SE),

where the stakeholder(s) define the needs and wants in the form of requirements. There requirements represent the expected behavior of a system based on how the stakeholder have written a statement based on their needs, and essentially state what is not desired in the system. Typically, the stakeholders define customer requirements (L0) which flows to the designers. Once the designers get the L0s they define top-level requirements (L1) and these requirements flow down to subsystem design engineers who define their subsystem requirements (L2) to satisfy the L1 requirement. This flow continues until the stakeholder and design agree that all system requirements are captured and implement correctly [8]. Once the requirements are defined and implemented at the component level, the system goes through integration, verification and validation process. This flow can be visualized using the systems engineering model known as the "Vee" model represented in Figure 4 [9].
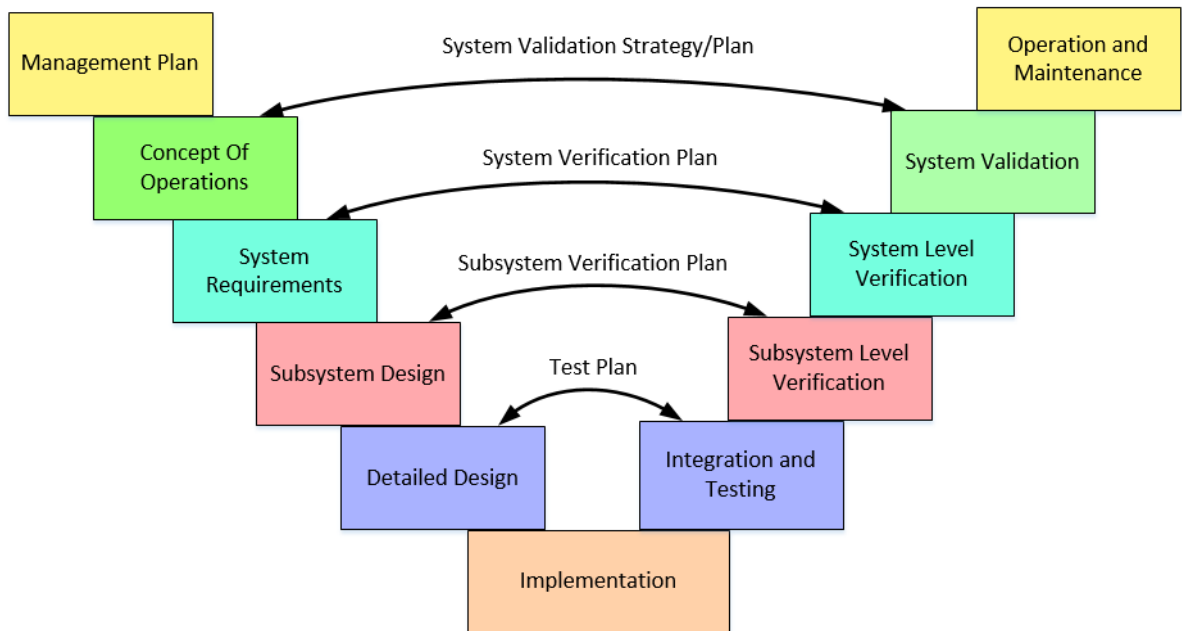
Figure 4: Systems Engineering Vee-Model

The requirements defined by the stakeholder act as proxies to their true preferences. To improve the capturing of the stakeholder's true preference the use of Value Based Design (VBD) is proposed, by using value functions to capture the true preferences of stakeholders [9,10,40,49]. Value functions are mathematical representations of the stakeholder's true preference and breakdowns a system design in terms of a value, typically in the form of monetary value [45,50].

In traditional requirements-based systems engineering a hierarchical description of the system is used to address interactions between subsystems [12,52,54]. This type of description arranges the system into levels, like a tree structure where each subsystem of the tree cannot communicate with each other until they reach the top level. This type of description works well for descripting the system architecture but it not the best way to show how the subsystems interaction with each other. A level four hierarchical decomposition of the Ares 1 is presented in

Figure 5 below as an example to show how the system architecture. As show in

Figure 5 there are multiple subsystems that can interaction with each other, typically LSCES can contain multiple couplings and be highly complexed. The use of a hierarchical decomposition alone is not enough to capture the highly complex coupling between the

subsystem. This is where Multidisciplinary Design Optimization (MDO) can be introduced to

aid the designer in understanding these highly complex couplings that occur in LSCES.
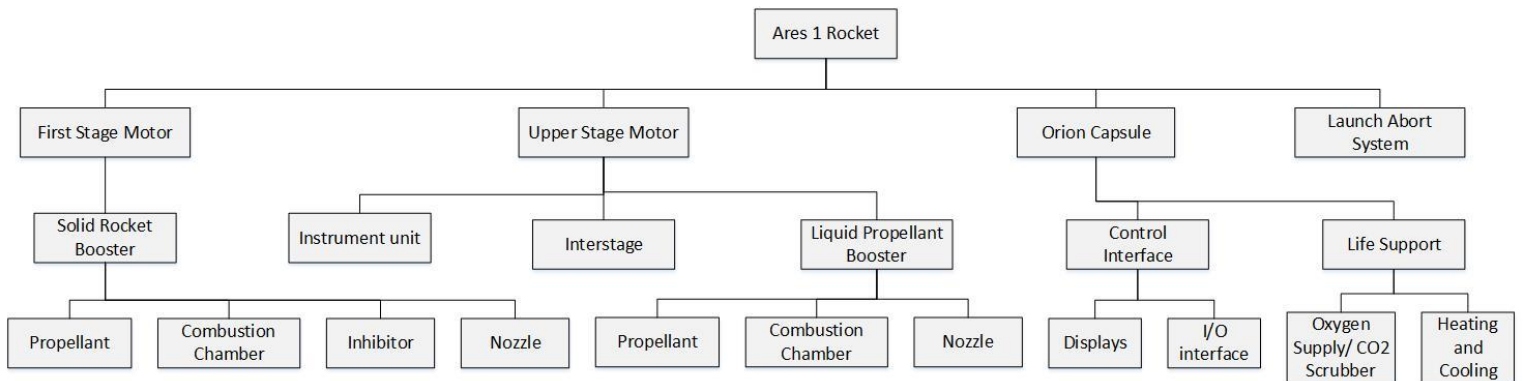
Figure 5: Hierarchical Decomposition of the Ares 1

Multidisciplinary Design Optimization

Multidisciplinary Design Optimization (MDO) was developed in the 1980's to

address interactions between subsystems during the design of LSCES. MDO captures

couplings between subsystems during analysis and optimization of a system's design [51,54].

With the use of computer simulations MDO is a powerful tool which can be used to improve

a system design. By incorporating MDO with today's technology LSCES composed of

multiple subsystems and couplings can go with the optimization process while maintaining

consistency in physics [13]. To better understand how this process works an example is

presented.

A typical engineered system can be broken down into disciplines or subsystems

where individuals focus on the area their expertise best suit the project [16]. Once each team

is creating each team begins designing their components. Once each team has a design they integration each subsystem design together to see if the design satisfies the customer requirement, if there are any issues in the integration the design is reevaluated and updated accordingly. This is done until the system has satisfied the customer requirements and has reach system convergence [13]. Figure 6 shows the flow of this process for a simple rocket design. An analysis is performed within each discipline, where design variables are varied to find the optimum design within each discipline. An "optimal" design can be found using the traditional method however the interactions between the subsystems is lost. To capture the interactions convergence must occur in each subsystem every time a design variable is changed or every time optimization program reaches its next iteration. Perform system convergence using the traditional method requires an enormous amount of computational hours which would not be feasible for designing LSCES.
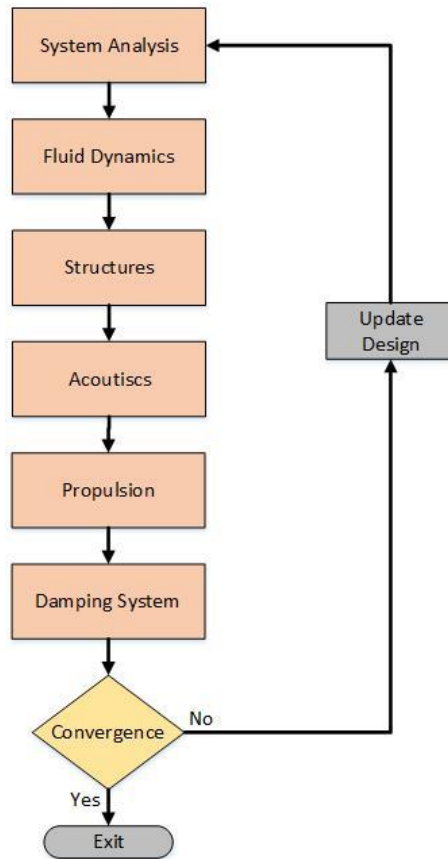
Figure 6:Traditional Optimization Method

Jaroslaw Sobieszczanski-Sobieski developed a way to address the loss of coupling information in hierarchical models, where subsystems are separate and not coupled together [14]. This approach focuses on capturing system couplings, analyzing how each subsystem affects the outputs of other subsystem they feed information into. The subsystem outputs are known as behavior variables, by capturing the behavior variables a subsystem a local linearized optimization problem can be used to determine how a change in one subsystem affects other subsystems. This approach can take advantage of sequential linear optimization of the system without losing information of subsystem couplings, shown in Figure 7.
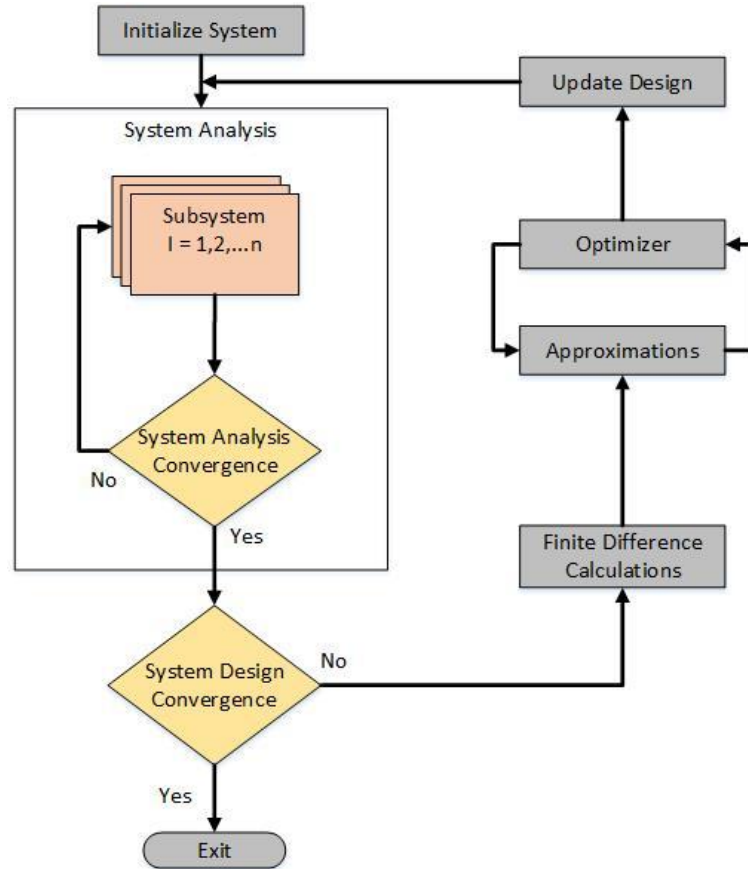
Figure 7:MDO Flowchart

The optimization problem begins with initialization of the system, then the information is categorized into its respective subsystems and sent through the system analysis. The subsystems are calculated using an iterative process until system analysis convergence, where the hierarchic sequence of the subsystems determines the CPU time until convergence. For instance, in the case where no subsystem feedbacks exist, the sequence only needs to be executed once for the system analysis to converge. However, is the system containing multiple subsystem feedbacks the CPU time required until convergence increase proportionally with the number of feedbacks. A simplistic way to view the number of feedbacks and feedforwards in the subsystem analysis is to use a Design Structure Matrix

(DSM) which will be explained in the next section. Once the system analysis is converged, a finite difference calculation is used to perturb the design and behavior variables within each subsystem and is sent through an optimization method to update the system design to a more preferred design. Approximations for the total impact these variables have on the system are then needed to account for the subsystem interactions, which would later be used to update the design. This process is done until an optimal design that satisfies the system design convergence is found.

<div align="center">Design Structure Matrix</div>

A Design Structure Matrix (DSM) is a simplistic way to represent subsystem interactions within a complex system by showing the feedforwards and feedbacks of each subsystems using a matrix structure [17]. Here the feedforwards and feedbacks are represented by connecting lines feeding from one subsystem to the next. The feedforwards shown in the top right and feedback is shown in the bottom left. Depending on the size of the DSM the visualization technique for displaying the interactions can vary. In the case of LSCES with many coupled subsystems the matrix can be represented with markers representing each coupling. Figure 8 and Figure 9 shows different ways to visualize a coupled system with five subsystems. $\bar{X}_{i,}$ in the figure represents the design variables which are independent variables used to define the subsystem. The $\bar{Y}_{i,}$ represents the behavior variables which are the outputs of the subsystem with respect to a particular design. The system shown in Figure 8 shows how a fully coupled system, meaning that the behavior variables of each subsystem impact their neighboring subsystems. The DSM takes the fully coupled system representing each coupling as dots which connects the lines that feed from one subsystem to the next, and the

design variables are arrows directly feeding into the subsystems. By using a DSM, the designer can easily visualize a LSCES, consisting of multiple subsystems with unique coupling patterns. Not only does DSMs make visualization easier, the designer can use a DSM to reorder which subsystems are calculated first in the optimization process to reduce the amount of CPU time needed[18].
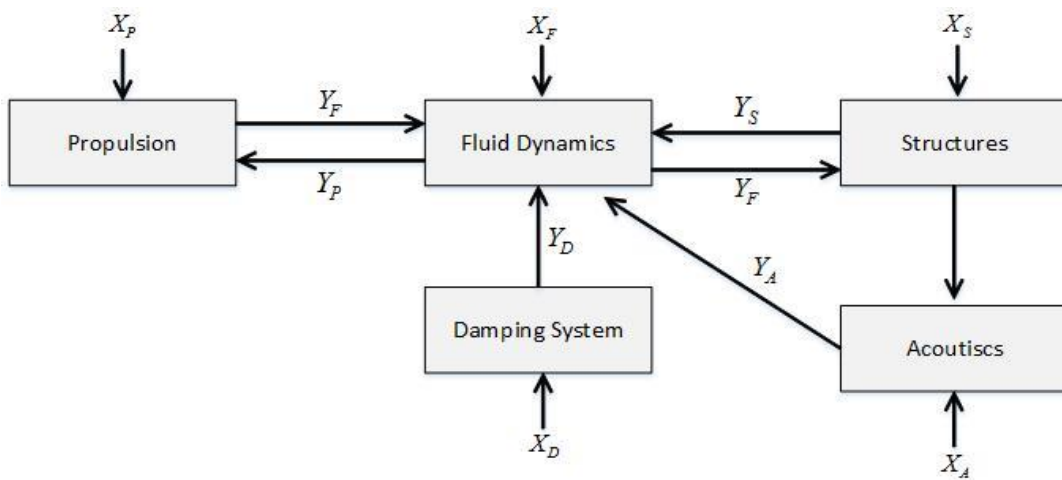
Figure 8: Coupled System (Spaghetti Graph)
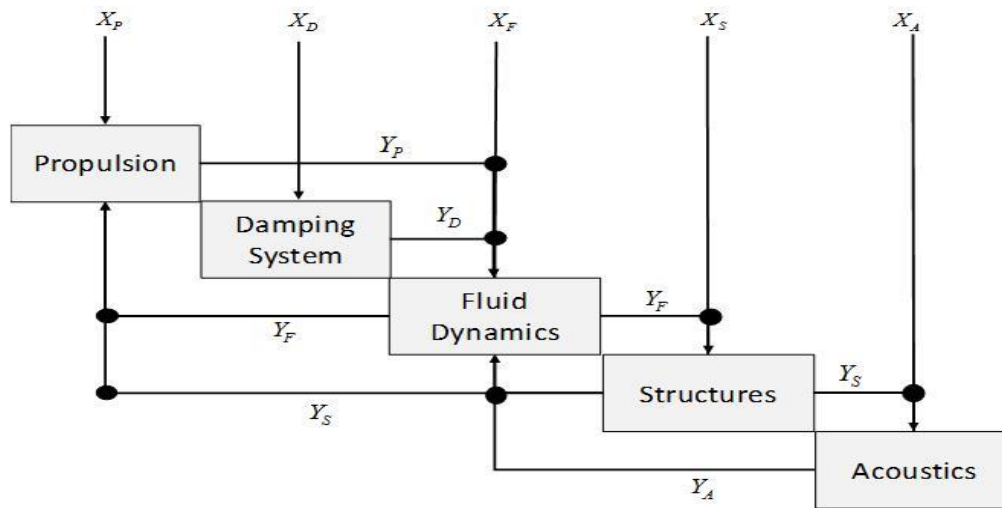
Figure 9: Design Structure Matrix of Coupled System

Global Sensitivity Equations

To determine overall system impact, sensitivities of subsystem couplings are analyzed through the implementation of a coupling strength analysis. The local and global derivatives are analyzed using the Global Sensitivity Equations GSE), which provides an efficient approach to obtain first order sensitivity of the systems behavioral response with respect to design variables [9-11]. This is done by decomposing the larger system into smaller subsystems and evaluating the subsystem behavioral responses. These system sensitivities are $\left(\frac{dY_A}{dX_A}, \frac{dY_A}{dX_B}, \frac{dY_B}{dX_A}, \frac{dY_B}{dX_B}\right)$ for the 2-subsystem example in Figure 10. These sensitivities are based on subsystem behavioral response sensitivities, $\left(\frac{\partial Y_A}{\partial X_A}, \frac{\partial Y_A}{\partial X_B}, \frac{\partial Y_B}{\partial X_A}, \frac{\partial Y_B}{\partial X_B}\right)$. The approach is aimed at solving the total derivative matrix of the system, which gives information on the influence of changes in one subsystem's output, due to changes in design variables within another subsystem.
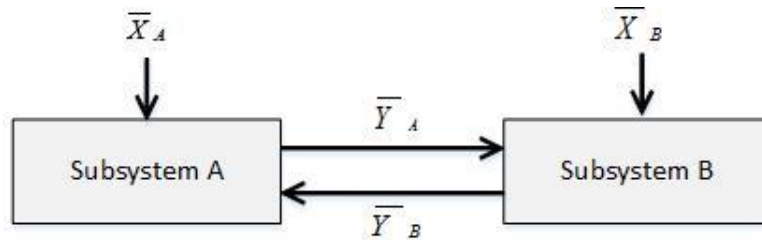
Figure 10: Coupled Subsystem Example

Here subsystem A and subsystem B are coupled together, where $\bar{X}_A$ and $\bar{X}_B$ represent the design variables going into each respective subsystem and $\bar{Y}_A$ and $\bar{Y}_B$ represent the behavior variables of its respective subsystem. The behavior variables also act as inputs to the opposite subsystems, i.e. $\bar{Y}_A$ will feed into subsystem B and $\bar{Y}_B$ will feed into subsystem A.

To find the total derivatives of the design variables a Taylor Series expansion is used shown by Eq. 1 and 2:

$$\frac{dY_A}{dX_A} = \frac{\partial Y_A}{\partial X_A} + \frac{\partial Y_A}{\partial Y_B}\frac{\partial Y_B}{\partial X_A} \tag{1}$$

$$\frac{dY_B}{dX_B} = \frac{\partial Y_B}{\partial X_B} + \frac{\partial Y_B}{\partial Y_A}\frac{\partial Y_A}{\partial X_B} \tag{2}$$

When the chain rule is applied, the last total derivatives are found using Eqs. 3 and 4:

$$\frac{dY_B}{dX_A} = \frac{\partial Y_B}{\partial Y_A}\frac{dY_A}{dX_A} \tag{3}$$

$$\frac{dY_A}{dX_B} = \frac{\partial Y_A}{\partial Y_B}\frac{dY_B}{dX_B} \tag{4}$$

Once the equations are derived they can be represented in matrix form shown by Eq. 5 below:

$$\begin{bmatrix} 1 & \frac{-\partial Y_A}{\partial Y_B} \\ \frac{-\partial Y_B}{\partial Y_A} & 1 \end{bmatrix}\begin{bmatrix} \frac{dY_A}{dX_A} & \frac{dY_A}{dX_B} \\ \frac{dY_B}{dX_A} & \frac{dY_A}{dX_B} \end{bmatrix} = \begin{bmatrix} \frac{\partial Y_A}{\partial X_A} & 0 \\ 0 & \frac{\partial Y_A}{\partial X_B} \end{bmatrix} \tag{5}$$

The left-hand side of the equations represents the sensitivity matrix, where the local behavior variables impact on a subsystem is captured. If a behavior variable changes in subsystem A its impact on subsystem B is captured with this matrix. The far-right hand side matrix represents the sensitivity of the subsystem behavior variables with respect to the subsystems design variables i.e. changes in design variables $\bar{X}_A$'s impact on behavior variable $\bar{Y}_A$. The total local derivatives are then solved for using matrix math to obtain the matrix shown in the center of the equation above. This matrix represents the total local sensitivity of a subsystem's behavior variables with respect to the design variables, including the coupling

sensitivity captured in the left-hand side matrix [52,53]. The local sensitivities within these matrices are typically found using a finite difference method.

The outputs found in the matrices can also vary highly by magnitude, as the units for most of the coupled systems won't match up. To get an accurate comparison of the strength these sensitivities have with respect to each other a normalization technique is used to normalize the left-hand side matrix. Below is an Eq. 6 which represents the normalized coupling sensitivity equation of the 2 subsystem example shown above:

$$\frac{\partial Y_A'}{\partial Y_B} = \frac{dY_A}{dY_B} \frac{Y_B}{Y_A} \tag{6}$$

Once normalized, the inverse of the matrix can be multiplied with the right-hand equation to calculate the total derivatives. To recover the true total derivative information, the normalization process should be reversed as shown below with Eq. 7.

$$\frac{dY_A}{dX_B} = \frac{dY_A'}{dX_B} \frac{Y_A}{X_B} \tag{7}$$

Local Sensitivity Coupling Strength Analysis

Once the local sensitivity information is captured a comparison of coupling strengths can be made. This information can be important to determining strong and weak interactions within the localized design space. Once solved the GSE equations shown above provide the normalized sensitivity information. A method to analyze the sensitivity of these couplings is by measuring the normalized local sensitivity information and running a comparative study where a larger number represents a stronger coupling. By comparing the couplings, the designer can get a general idea of the relative strength of each coupling within the local design space [19,53]. The designer can then select the couplings that are weak with little

impact on the problem and consider elimination or suspension to save on computation time.

This method is used later to determine the coupling strengths that impacted T/O on the Ares

1.

CHAPTER 4

DEVELOPMENT AND VERIFICATION OF ARES 1 META-MODEL

Initial methods for recreating the thrust oscillation event included the use of coupling a CFD program known as Star CCM+ with a FEA program known as ANSYS Workbench. The idea was to use Star CCM+ to gather pressure data and create a forcing function that can be placed on the structures of the rocket in ANSYS. The structures program would then calculate our deflections and we would then take these deflections and reiterate them back into the CFD Program. This approach turned out to be heavily taxing on time and riddled with numerous errors, such as meshing errors when placing the deformed ANSYS model back into the Star-CCM program. A new approach was proposed by using a meta-model based on numerical approach to determine the values of pressure along the walls of a RSRM during a certain range of time [36]. The following equation is used in creating a numerical model for the pressure oscillations.

$$p_i(t) = \sum_j p_{ij} \sin(2\pi f_{ij} t) + rand([0:1]) * (P_{high} - P_{low}) \tag{8}$$

Where, $f_{ij} = \frac{S_{ij} U_i}{L_i}$

Where p_{ij} is the initial pressure on a grid i by j, f_{ij} is the vortex shedding frequency, and t is time. The vortex shedding frequency is determined using the 2nd part of the equation, where S_{ij} a value that determines how oscillatory the flow is, L_i is the length of the obstacle protruding into the flow, and U_i is the velocity of the fluid. Here we added randomize to achieve output similar the output from Star CCM since it was not a perfect sinusoidal wave.

A random pressure between a range of P_{high} high pressure and P_{low} low pressure outputted by Star CCM.

It is desirable to determine the impact that pressure oscillations have on the thrust produced by the solid rocket motor. So a mathematical model presented in research conducted by Dr. Fred S. Blomshield to approximate Thrust Oscillation due to multiple rocket instabilities is used to relate pressure oscillations to T/O [37]. In the past it was assumed that to approximate thrust oscillation due to pressure oscillation, one needs to multiply the nozzle area by the peak-to-peak pressure oscillation [37]. These methods yield smaller oscillations than what occurs inside the solid rocket motor. Using the following equation assuming that longitudinal oscillations have a higher impact on thrust oscillation and the transverse modes cause no thrust oscillations the magnitude of T/O can be found. [37]

$$\Delta F = 2A_c \Delta P \tag{9}$$

$$\Delta F = [F + P_A A_E - (\overline{P_N} + \overline{P_H})A_C \frac{\Delta P}{P_N} \tag{10}$$

The first equation is a simplified version only considering the peak-to-peak pressure oscillation and the motor's chamber area. The second equation considers not only the peak-to-peak pressure oscillation but also motor's chamber area, ambient pressure, head-end pressure, nozzle pressure, nozzle exit area and the thrust produced by the solid rocket motor.

Using the initial simulation, we can determine the vortex shedding frequency along with the initial pressures that occurs within the SRM at time 0. With the initial data the meta-model can be created to calculate the behaviors of each discipline that is effected by T/O or effect T/O. The meta-model structure is shown by Figure 11, where the main drive is the

"Fluid Dynamics" section of the meta model. This section acts are the driver for the other sections as it receives and sent out data to the other sections of the model.
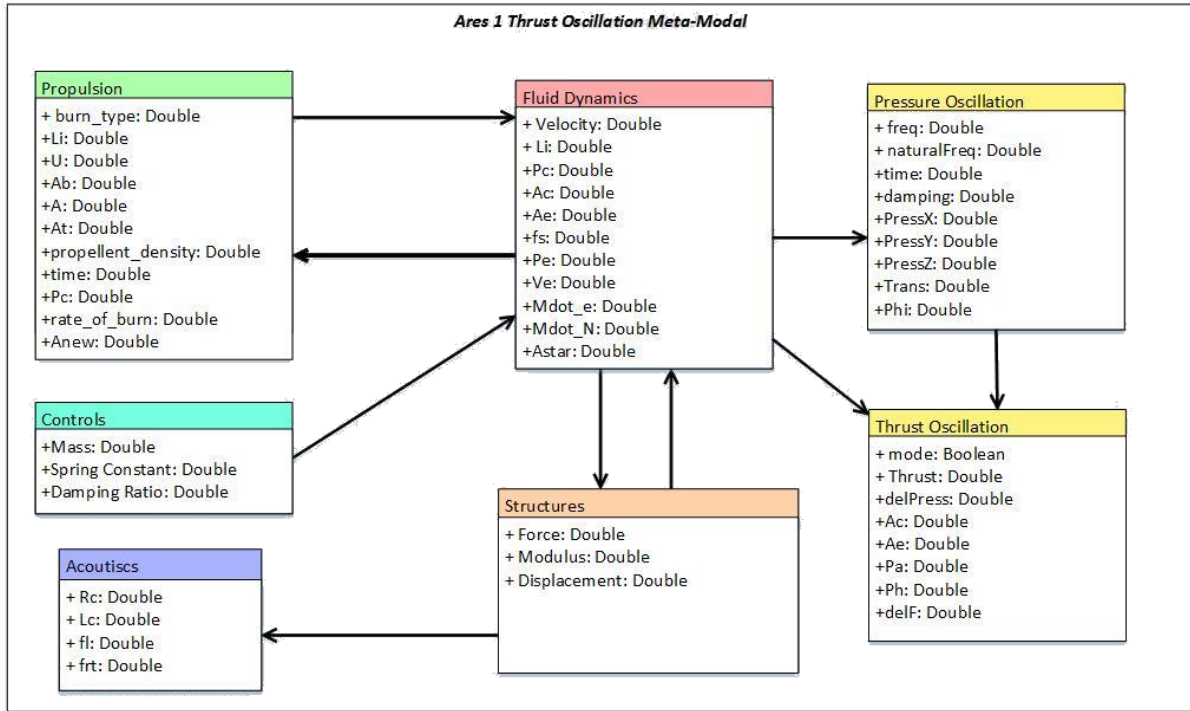
Figure 11: Metamodel Diagram

In order to understand how the Metamodel functions, it is important to understand the mathematical calculations that lead up to the calculation of T/O. Each subsystem is broken into disciplines, which are "Propulsion", "Acoustics", "Fluids", "Structures", and "Controls", with additional subsystems that help calculate T/O. In Chapter 3 Propulsion, Acoustics, Fluids, Structures, and Controls were discussed in detail at the system level, here will introduce the mathematical formulae used to model each subsystem.

The propulsion subsystem is modeled as a SRM with a star grain for the burn area. This is used to make the analysis simple as a star grain gives a constant burn over time.

Since, the foucs of the subsystem is to determine the effects of the changing changing

pressure and the burn rate the model will use the following equations. These equations

produce P_c pressure in the chamber and r burn rate which can be used in understand how

propulsion properties of the SRM effect T/O. Here the equations used are assuming that the

rocket is an end-burning rocket instead of an erozive burning rocket.

$$r = ap^n \tag{11}$$

$$P_c = \left[aC^* \rho_p \frac{A_b}{A_t} \right]^{\frac{1}{1-n}} \tag{12}$$

Here, p, ρ_p, A_b, and A_t is the fluid pressure, propellent density, burn area, and area at the

throat of the nozzle, and a, and n are empirically determined constants. Also, C^* is defined

by the following equation.

$$C^* = \left(\frac{\gamma+1}{2} \right)^{\frac{\gamma+1}{2(\gamma-1)}} \sqrt{\frac{RT_t}{\gamma}} \tag{13}$$

Where, R and γ are gas parameter constants, and T_t is the total temperature inside the SRM's

chamber.

The controls subsystem is modeled as a spring-dampener system, where the spring is

placed at the end of the first stage SRM. Here, the spring is attached to a fixed end and to the

first stage SRM while a forcing function represented by $F(t)$ is applied to the first stage

SRM. The spring's objective is to damped out the forces being applied to the structre, the

amount of force being damped is determined by the spring constant k and the dampener c.

Figure 12 shows a simple example of a spring-mass system, where the mass is subjected to a

force and moves towards the left side. The spring wants to prevent the mass from touching

the wall and wants the mass to reach its equilibrium state without causing more oscillations.
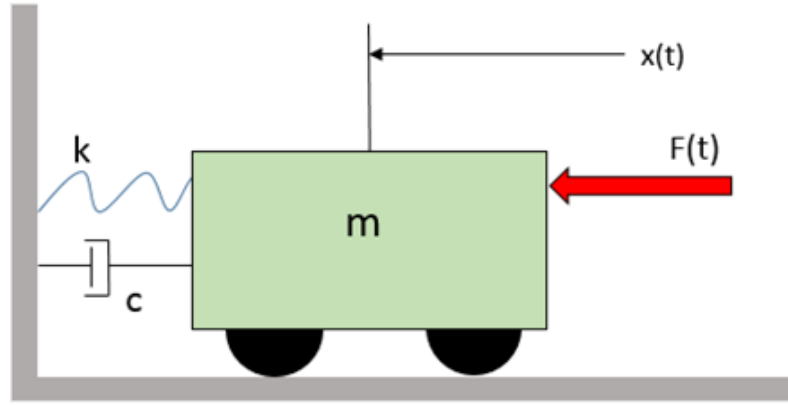
Figure 12: Simple Spring-Mass System

Based on the design of the spring, the damping ratio of the spring can be calculated using the

following equation.

$$\zeta = \frac{c}{2\sqrt{mk}} \tag{14}$$

Once the damping ratio is known transmissibility can be used to calculate damped

force that is applied to the structure. Transmissibility is the capability of an external force to

impact an oscillatory response of a system through the proximity to its resonance frequency

[24]. Eq. 12 below describes this processes and shows how frequencies close to the

resonance of a system can have a significant impact to the creation of a large amplitude

response.

$$T = \frac{F_T}{F_O} = \frac{\sqrt{1+\left(2\zeta\frac{\omega_i}{\omega_n}\right)^2}}{\left(1-\left(\frac{\omega_i}{\omega_n}\right)^2\right)^2 + \left(2\zeta\frac{\omega_i}{\omega_n}\right)^2} \tag{15}$$

Where F_T represents the force as a function of frequency, F_O is the original force magnitude, ζ is the damping coefficient, ω_i is the vortex shedding frequency, and ω_n is the acoustic mode.

As the frequency generated by an external force approaches the resonance frequency of the system its transmissibility goes to infinity, this is where the system will have the greatest oscillatory responses.

Modeling of the acoustic subsystem is done numerically determining the acoustic mode frequencies of the SRM. The analysis is done by assuming the cavity of the SRM is acoustically closed despite the exit area coming into contact with the external environment [20]. The assumption needs to be made for the theoretical method to be used. As mentioned before there are three main acoustic modes within a closed environment, they are the longitudinal, tangential and radial modes shown in Figure 3. All three acoustic modes may contribute to acoustic instabilities within engines, however the longitudinal modes are the main focus. To note even though the focus is the longitudinal mode, the tangential and radial modes show higher instabilities at higher frequencies [21]. The Ares 1 was shown to have had very low acoustic and resonance frequencies associated within the

SRM [48,49]. To simplify the problem the radial and tangential acoustic modes will be neglected in the model as they are more associated with higher frequencies, which did not show any contribution to T/O in the Ares 1. The longitudinal frequencies of the SRM are calculated using Eq. 17 [22].

$$f_{lmn} = \frac{c}{2\pi}\sqrt{\frac{k^2\pi^2}{L_c^2}} \qquad (16)$$

In Eq. 11 c is defined as the speed of sound, LC is the length of engine chamber, and k is the longitudinal acoustic modes. Speed of sound is dependent on the temperature and properties of the surrounding gas and is described by Eq. 18 below.

$$c = \sqrt{\gamma RT} \tag{17}$$

Here in Eq. 12 is defined as gamma, which represents the ratio of specific heats, Represents the gas constant, and T represents the temperature of the gas.

Higher temperatures and density play a major role in determining the speed of sound in a specific medium [24]. In this case a temperature of 20 degrees Celsius and gas constant of 1.4 is used to give a speed of sound of 343 m/s. With all variables accounted for, Table 1 showcases the natural frequencies of the Ares 1 meta-model:

Table 1: Acoustic Mode Frequencies for Ares 1 SRM chamber

Acoustic Modes	SRM Acoustic Frequency
1L	19.7937 Hz
2L	39.5875 Hz
3L	59.3812 Hz

Structures Modeling

With the acoustic mode frequencies captured and compared with the vortex shedding frequencies, pressure oscillations can then be generated and placed onto the interior walls of the SRM as forcing function. Originally, the structures model was simulated in ANSYS workbench [33]. However, to save on computational time, a meta-model was created using sampled data collected by running the ANSYS analysis multiple times. This was done by changing the loading and material properties applied to the model. A total of nine variations

were used to create a forcing function that fits the structural behaviors of the system. Eq. 19 shows how the pressure oscillation loads on the SRM were captured [24].

$$f(t) = F_o sin(\omega t) \tag{18}$$

In Eq. 19 F_o represents the magnitude of the force, ω represents the driving frequency and t represents time. Here, the magnitude of the force is calculated in the "Fluids" section of the meta-model shown in Figure 11.

Now that all of the disciplines were model numerical and placed inside the metamodel, it was tested against the Star-CCM+ to ensure accuracy. Figure 13 below showcases the loads captured by the numerical metamodel compared with the loads captured in a simplified Star-CCM+ model.
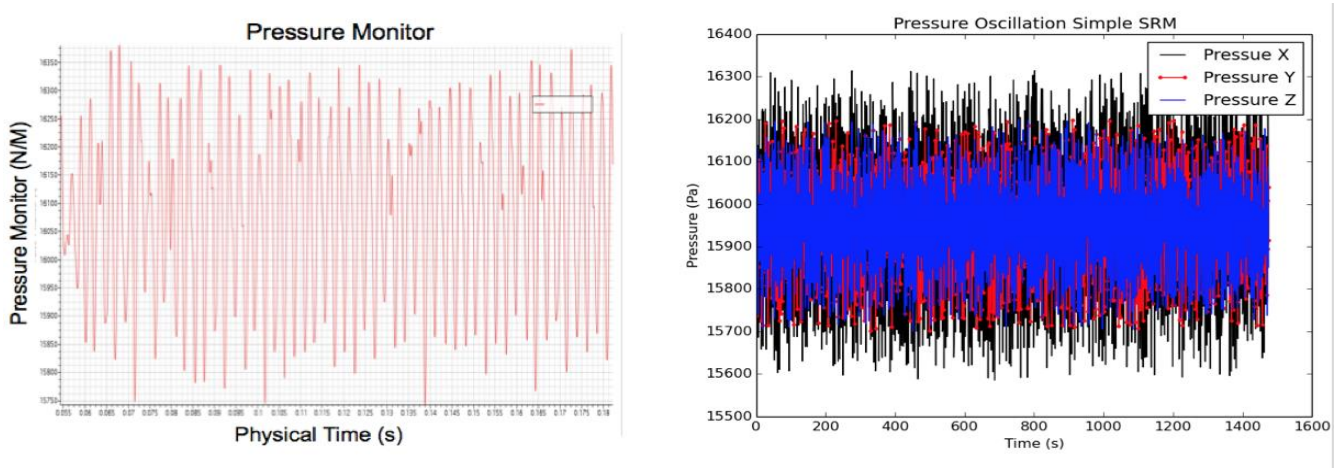

Figure 13: Pressure Oscillation Star CCM (left), Pressure Oscillation meta-model (right)

CHAPTER 5

UNCERTAINTY COUPLING ANALYSIS

During operation, some LSCES may have unstable behaviors during operation, (i.e. turbulent flow, abnormal vibrations, etc.) this makes it challenging to understand how all the subsystems will interact with each other under these unstable behaviors. To investigate these issues uncertainty is added to the coupling strengths analysis, to provide more detail on how subsystems interact with each other based on unstable behaviors and uncertainty in the MDO process[56]. Here, the T/O event that occurred during the operation of the Ares 1X will be should to show how uncertainty and instability can affect the couplings between subsystems.

Before uncertainty coupling analysis is introduced, it is important to understand uncertainty based optimization. It has been around since the 1950s and continues to grow within multiple research areas [56,57]. Focusing in aerospace engineering the main disciples examined were, structures, aerodynamics, and controls each closely coupled together where uncertainty impacts are cross propagated [58]. With the desire to take a holistic approach in solving multidisciplinary uncertainty design problems, UMDO was introduced into academia. UMDO improves the design process by benefiting from the synergistic effects of coupling disciplinary optimization. By taking uncertainties into consideration in the design phase, UMDO can closely simulate a realistic system. To closely represent a system UMDO utilizes both system modeling and uncertainty modeling. Where system modeling includes the mathematical modeling of the system and its disciplines. Within this model the design variables, objective function and behavior variables are defined. This model captures the underlying physics, ensuring the design does not violate any laws of physics or violate any

constraints. The uncertainty modeling involves the quantification of uncertainties within the system design. There are many mathematical theories and method already developed to model uncertainty [59], there is probability theory, evidence theory, etc. Throughout the lifecycle of any aerospace system there exist a vast number of uncertainties. Therefore, to minimize unacceptable calculation burdens it is necessary to use sensitivity analysis to filter out factors that have no significant influence on the system design [2]. Combining both systems modeling and uncertainty modeling, UMDO is developed. However, the UMDO procedure is about how efficiently organized and realized UMDO computer scripts created by the designer [60]. However, for this research the main area of interest is the uncertainty within the system's disciplines so a modified flowchart is shown below, the major steps include sampling the design variable in the design space, perturbing that variable and performing a coupling analysis to determine how each coupling changed with the change in the design variable.
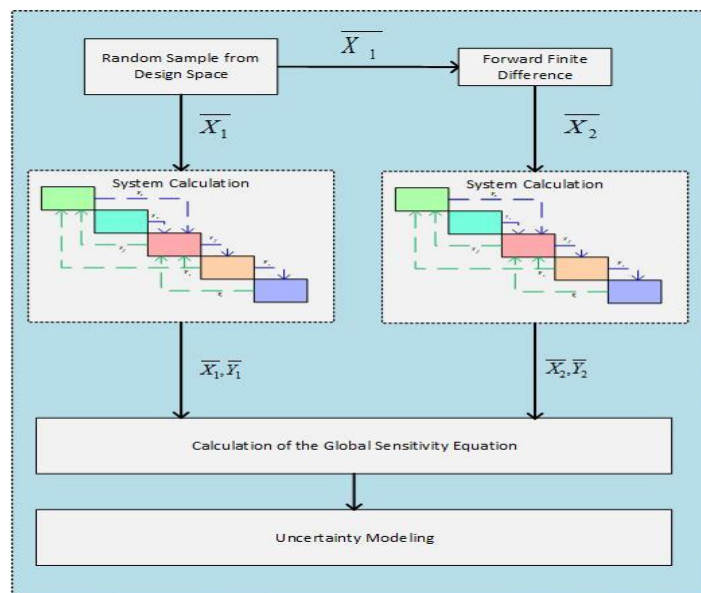

Figure 14: Uncertainty Analysis Flowchart

Using a coupling analysis with uncertainty the impact of unknown oscillations in behavior variables can be approximated to provide a better understanding of how the subsystem interactions of a large-scaled complex engineered system behave under unstable phenomena such as thrust oscillation. The analysis presented in this paper produced six Monte Carlo simulations, which contains the same logic but samples one design variable. Each Monte Carlo simulation samples the design variable, perturbs that samples and calculates each subsystem's behavior variable based on the original sample and the perturbed sample. Once the behavior of the sampled and perturb design variable is known, forward finite difference is used to determine how each coupling changes with respect to the interactions of the subsystems. Along with the calculations of see how each coupling changes, the change in subsystem variables and design variables is also calculated. To produce accurate results each Monte Carlo analysis takes one million samples uses forward finite difference and feeds the information into Global Sensitivity Equations (GSE) and plotted the vitality of each coupling in the $\overline{A}$ matrix to see how the sensitivity of each coupling showing the varying uncertainty in the model. Once all the Monte Carlo simulations finished all of the samples were stored and the trends of each coupling were captured as histogram plots. This is shown in Figure 15, it was noticed that each coupling shared a similar trend while changing each design variable independently. Therefore, the plots shown in Figure 15 are focused around the length of the inhibitor which is a design variable which displayed high levels of impact on T/O due to changes in the vortex shedding magnitude. If a plot was not shown in Figure 15, it was because the trend of the coupling was either focused around zero or a certain value. The trend of each of the four couplings presented in Figure 15 show that zero has the highest

frequency, however if the each plot is examined the coupling has a higher tendency of being strong or weak. To better understand if the coupling is strong or weak Figure 15 show the average coupling strength values for each subsystem interaction based on the samples used in the each of the Monte Carlo simulations. Based on the information in Table 2 every subsystem that interactions with the fluids subsystem in strong in magnitude meaning that little changes in each subsystem has a major impact on T/O. However, the interactions from T/O back to the other subsystems is weak, meaning that T/O is not driving any changes in the system, it is driven by all subsystem interactions. All the zeros in Table 2 represents no coupling change with the changes in the design variable. As show any subysytem that interations with the acoustic subsystem has a zero, this is do to the fact that acoustics in determined based on the geometry properties of a closed system. In this case that closed system the is the solids rocket motor's chamber . There is one coupling that is only affected by a change in the length of chamber design variable and that is acoustics feedback on structures, this is due to the fact the analysis is only focused on the longitudinal modes.
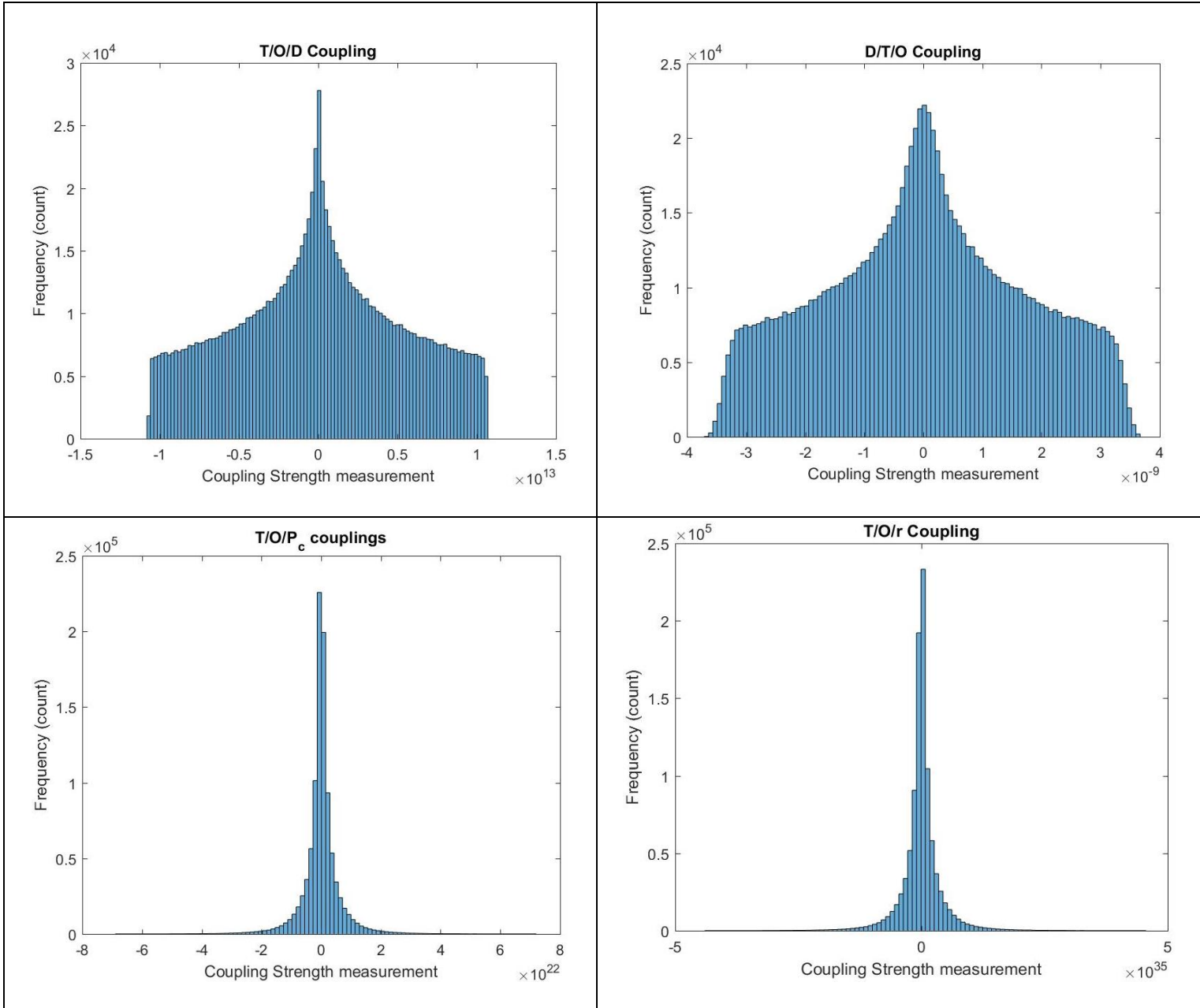
Figure 15: Uncertainty in coupling with change in length of inhibitor

Table 2: Coupling measurements for each design variable

Average coupling strength measurement						
	L_i	U	R_c	L_c	R_e	R_b
$\dfrac{T/0}{D}$	-1.1E+13	-1.07E+13	-1.1E+13	-1.32E+13	-1.1E+13	-1.1E+13
$\dfrac{T/0}{f_a}$	-1.3E+14	-6.34E+14	-1.1E+14	0	-9.4E+13	-1.5E+15
$\dfrac{T/0}{P_c}$	-7.0E+22	-2.12E+22	-9.78E+21	0	-9.7E+21	-2.75E+23
$\dfrac{T/0}{\zeta}$	-5.0E+26	-1.17E+26	-3.87E+25	0	-1.2E+26	-1.67E+25
$\dfrac{T/0}{r}$	-4.5E+35	-1.34E+35	-6.19E+34	0	-6.2E+34	-4.6E+35
$\dfrac{D}{T/0}$	-3.67E-09	-4.17E-09	-4.40E-09	0	-4.59E-09	-4.0E-09
$\dfrac{D}{f_a}$	0	0	0	-0.0035	0	0
$\dfrac{P_c}{T/0}$	-5.16E-16	-7.10E-17	-2.73E-16	0	-3.55E-17	-3.11E-15
$\dfrac{r}{T/0}$	-8.15E-29	-1.12E-29	-4.31E-29	0	-5.61E-30	-3.31E-28
$\dfrac{D}{P_c}$	-3.40E-07	-1.95E-07	-2.26E-06	0	-4.60E-07	-1.65E-05
$\dfrac{D}{r}$	-5.37E-20	-3.08E-20	-3.57E-19	0	-7.26E-20	-1.20E-18

To visualize how each coupling compares to one another Figure 16 gives a visual representation of all system couplings and their relative impact, this plot is indented to compare each coupling together. Therefore, each coupling value was rescaled to a value from zero to five. Here, the x-axis is the coupling strengths' measured value while the y-axis is the probability of the value occurring during system operation. Comparing each coupling the system designer can determine which couplings need to be further analyzed to improve overall system behavior. In this example the system designer would want to focus on couplings that range between the magnitudes of 2 to 6, trying to update the system design to decrease the probability of T/O from occurring. The trends and probability of each coupling are presented in Figure 16. By analyzing the likelihood of the coupling being strong or weak an approximation can be made on the 'true' impact of that coupling and a more accurate behavior of the subsystem can be modeled. Therefore, the value of the system can be calculated with uncertainty included.
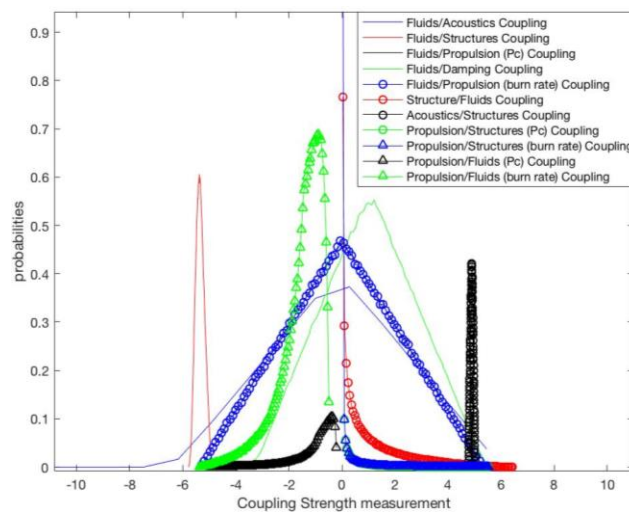

Figure 16: Uncertainty coupling analysis

CHAPTER 6

VALUE MODEL ANALYSIS WITH UNCERTAINTY

Ares 1 Value Model

To determine how much value, the 1st stage T/O event effects the overall mission success a resupply mission to the ISS is developed. The mission is broken down into two segments, the first being the first stage rocket motor that has been the main focus of this research, and the second being the J-2X upper stage rocket engine. The design of the J-2X will remain a constant, where the mass of the engine is 2470 kilograms and thrust is 1310 kilonewtons [41,45]. Since, this design is treated as a 3 stage rocket the total velocity need to get to the ISS needs to be calculated. Once the total velocity is known the velocity produced by the J-2X engine can be subtracted from the total velocity and the 1st stage SRM required velocity to complete the mission can be calculated. Once known the required velocity can be compared with the current design to see if the mission will be successful.

To determine the value of the 1st stage SRM design the key design and behavior variables impacting mission success are identified. Once mission success rate is found, the cost associated with the mass of the structure and the propellant can be found. The value function is now in terms of dollars and the mission success rate. To capture the mission success in terms of dollars the mission success rate will be used as a multiplicative term to capture the revenue made from delivering the payload safely. For the case presented in this paper delivering 1 kilogram to the ISS returns $22,000. The initial design and behavior variables shown in Table 16 will be used to calculate the Ares 1 value.

Table 3: Design and Behavior Variables of the Value Function

Design Variables		Behavior Variables	
L_{it}	Length of Inhibitor	T/O	Thrust Oscillation
U_f	Velocity of Fluid	ΔV	1st Stage velocity
R_c	Radius of Chamber	M_s	Mass of Structure
R_e	Exit Radius	M_p	Mass of Propellant
P_c	Pressure of Chamber	A_1	First Acoustic Mode
L_c	Length of Chamber		

Since, profit is the true preference of the stakeholders and dollars can be understood across multiple areas the value function is represented as profit, where higher the mission success rate and lower the cost, the greater the profit. [42,46]. This function is a combination of mission success rate, analysis time, and T/O. Where the value function is captured by the revenue and cost defined by the following equations:

$$Value = Revenue - Cost_{total} \tag{14}$$

Where,

$$Revenue = P(MS) * Mass_{payload} * Price_{payload} \tag{15}$$

$$Cost_{total} = Cost_{system} + Time_{D\&D} * Wage_{Engineer} \tag{16}$$

Here, revenue is the multiplication of the mission success rate, mass of payload and the price charged to the customer to launch the payload, while the cost is the cost of system materials added with the amount of time spent in design and development multiple with the current engineering wage. Once the general basis and understanding of the value function is known, the Ares 1 value information can be added with the Congressional value model to determine the overall profit.

Congressional Value Model

While missions to space play an important role in the development of current

economical and technology develops the government needs to justify which programs get

funded. In this case the government is simplified using a model called the JFK model talked

about in "The Case For Mars"[61], where the data from the race to the moon help determine

if investing a mission to Mars benefits the economy. In regards to the Ares 1 project

investors, where the investors is the government, are investing towards the cost of the Ares 1

system itself along with any additional cost needed during the development process of the

system which is used towards the mitigation any unintended consequences. This test case

focuses on the Thrust Oscillation event as the major consequence that occurred during

operation. The Thrust Oscillation mitigation team was developed to mitigate the event and

added additional cost towards NASA overall budget during 2006-2010. The cost of the Ares

1 system is around 6.445 Billion USD, this includes design and development costs. To

determine the return of investment the total cost is calculated by adding the cost of the Ares 1

along with the T/O mitigation cost. Since there is a probability of the rocket surviving the

T/O event without additional cost required to design and develop mitigation devices such as

(example) the mitigation cost can be assumed zero. This can be expressed by the following

equation.

$$Cost_{total} = Cost_{system} + Cost_{mitigation} * P(TO) \qquad (17)$$

Knowing the cost, we can determine the possible return on investment assuming

investors are willing to invest their assets to equal that of the project's total cost. The investor

is expecting a 7$ return for every dollar invest into the project[61,62]. The investor is

gratitude the minimum return rate however, if the systems fails the return rate may decrease and there is a probability that if he/she is willing to invest more assets towards additional cost their return rate can increase. Let's examine the Ares 1 T/O issue, if the T/O event occurs and there is a need for additional cost then investors might invest more assets expecting a higher return on investment. However, if the mitigation cost is needed and the mitigation devices/plan fails then an assumption is made that the investor does not receives any additional return on investment due to failure. This information can be used to determine that if T/O does not occur then there is no need for additional resources and the return on investment remains the same. However, if the additional resources is needed and there is failure then the return on investment only includes half of the return rate of the Ares 1 system's value. This is due to return investment impacting education. This can be expressed by the following equation.

$$Value = Value_{Techology} + Value_{education} + Value_{Mission} + Value_{future} \tag{18}$$

$$Value_{Techology} = 0.1 * ROI \tag{19}$$

$$Value_{education} = 0.2 * ROI \tag{20}$$

$$Value_{Mission} = (0.6 - 0.4 * P(MS)) * ROI \tag{21}$$

$$Value_{future} = (0.1 - 0.05 * P(MS)) * ROI \tag{22}$$

$$where, ROI = (Return_{rate} * Public_{opinion}) - Cost_{total}$$

Where congress is broken down into four categories; education, technology, Mission Success, and future programs. Each category provides a unique value gain to the overall congress value, and they are broken down as follows[62]:

- Education → Value gained by developing the system and R/D work

- Technology → Value gained by the any technological spin-offs

- Mission Success → Value gained by the success of the system

- Future programs → Value gained by using the current program to plan future programs

Uncertainty within Value Function

While the uncertainty of within each coupling strength was calculated, each of the two value models proposed was analysis to see how uncertainty effected the overall system value. The goal of the analysis is to determine the average value of the system. Therefore, the one million samples that was used to calculate the coupling strength information is propagated into the value function. Each sample determines the systems value and once all the samples are collected an overall system value can be determined. This overall system value is an approximation based on all the data collected during the analysis, mainly determined by the average value among all of the samples. This is shown in Figure 17: Ares 1 Value model with uncertainty analysis (left) Congress value model with uncertainty analysis (right) where the graph to the left is the Ares 1 value model and the graph to the right represents the congressional value model. The two graphs shows the value of the Ares 1 system along with how much congress benefits from investing in the Ares 1 mission. Based on Figure 17: Ares 1 Value

model with uncertainty analysis (left) Congress value model with uncertainty analysis (right) a

summary of results is shown in.

Table 4: Value Model Summary

Parameter	Expected Value
Total value($M)	300 to 690
Total value with the highest Frequency ($M)	410
Congress return on investment ($M)	100 to 200
Congress return on investment with the highest Frequency ($M)	140
Ares 1 Value ($M)	300 to 690
Ares 1 Value with the highest Frequency ($M)	270

Here the results show what the expected profit is for the overall program along with what the

return on investment is for Congress. To infer on the data the Ares 1 program is expected to

produce a value around 270 million USD, this is the value that had the highest frequency.

With the Ares 1 producing a value of 270 USD million congress is expected to get a return of

140 million USD. To note that the total value of the system is the addition of the

congressional and Ares 1 value, therefore the total value is 410 million USD. This result

shows the total benefit each party gains from the success of the Ares 1 program.

Table 5: Summary of Congress Breakdown

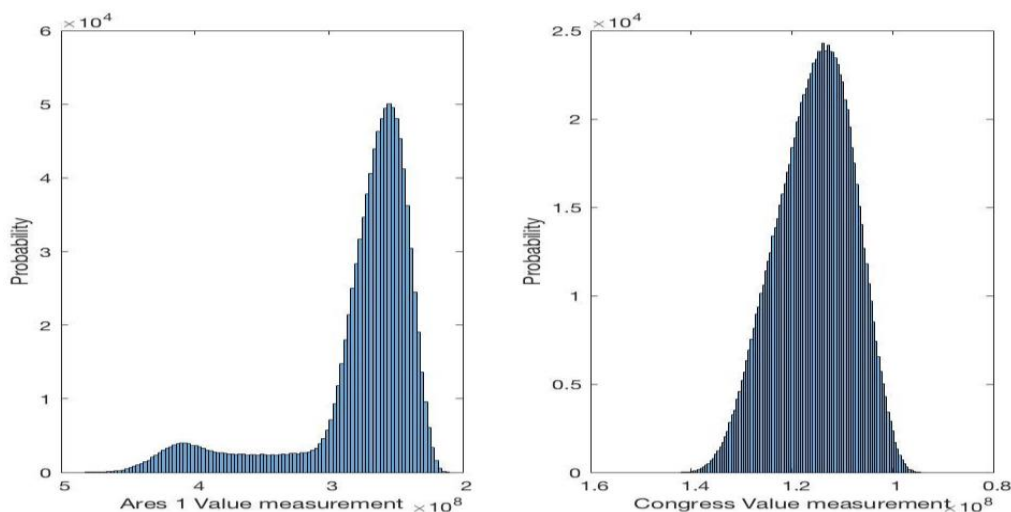| Area of Interest	Expected Value
Education value ($M)	25
Technology ($M)	18
Mission Success ($M)	82
Future Programs ($M)	15

Figure 17: Ares 1 Value model with uncertainty analysis (left) Congress value model with uncertainty analysis (right)

To further understand the benefit congress gains from investing into the Ares 1 program the congressional value function is broken down into four categories; education, technology, Mission Success, and future programs. To keep the units of the value model consistent and to provide a model that can be easily understood the congressional values above are represented in USD. Figure 18 shows the max, min and average values each area of interest produces based on Congress investing into the Ares 1 program. Here, the focus is on the average values, since this value has the highest likelihood of occurring. To infer on Figure 18 the four Ares of interest produce different amounts of value based on the success of the Ares 1 mission. Some of this values are held at a fixed minimum, stating that each area produces a certain amount of value even if the mission fails [62]. Based on the previous statement an assume of minimum funding for each area is assumed. Here education produces a minimum of 20%, technology a minimum of 10%. However, mission success and future programs are determined by the success of the mission
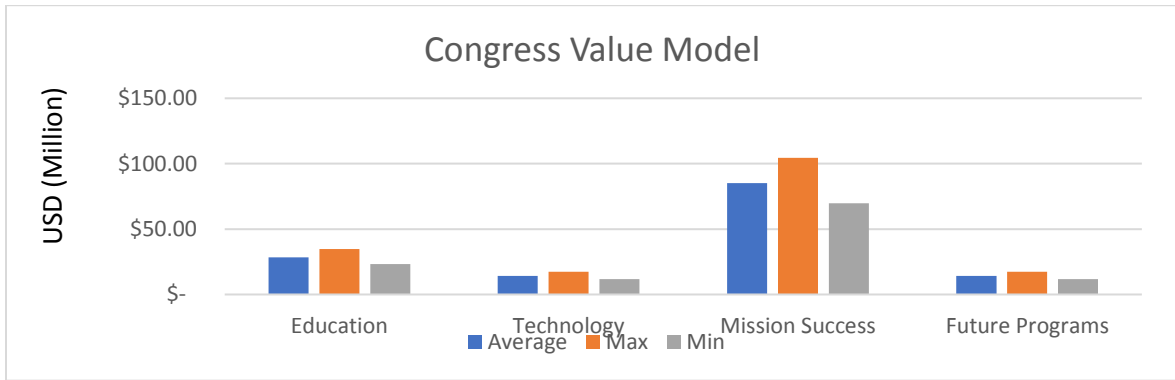
Figure 18: Congress's return on investment breakdown

With the overall value of both the Congress model and the Ares 1 model known, the value change can be determined using the average changing in each coupling strengths. To perform this analysis all other couplings are held fixed besides the coupling of interested. By doing this the change in value can be isolated with the change in coupling strength measurement. Similar, to the analysis to find the uncertainty in each coupling strength measurement, six Monte Carlo simulations were used to determine how each coupling affected the value with respect to their design variables. The results from each simulation are shown in Table 6, where the value in each cell is the value measurement change with respect to each coupling shown in the far left column, the rows represent each Monte Carlo simulation ran for each design variable. Based on the results from Table 6 the main couplings that impact value are

$\frac{T/0}{D}$ and $\frac{D}{T/O}$ when changing the length of the inhibitor. However, when change the chamber

dimensions $\frac{T/0}{fa}$ and $\frac{D}{fa}$ also have a high impact on the value. The other couplings have a

moderate impact on the system value.

Table 6: Average change in value with respect to average coupling measurement

Average change in value with respect to average coupling measurement $M (USD)						
	L_i	U	R_c	L_c	R_e	R_b
$\dfrac{T/0}{D}$	212.64	-16.19	26.065	0	6.57	216.94
$\dfrac{T/0}{f_a}$	21.18	26.82	-82.858	0	12.019	-62.87
$\dfrac{T/0}{P_c}$	-48.665	-26.106	33.802	-0.9135	16.73	-11.114
$\dfrac{T/0}{\zeta}$	4.513	9.11	-10.36	0	3.533	4.5687
$\dfrac{T/0}{r}$	-48.67	-26.106	33.802	0	16.7299	0.9483
$\dfrac{D}{T/O}$	-215.349	13.477	-28.7823	0	-9.2886	-219.6558
$\dfrac{D}{f_a}$	0	0	0	57.149	0	0
$\dfrac{P_c}{T/O}$	45.958	23.3967	-36.519	0	-19.448	-7.288
$\dfrac{r}{T/O}$	45.958	23.3967	-36.5193	0	-19.447	-2.4688
$\dfrac{D}{P_c}$	-12.114	6.027	15.771	0	-31.812	-51.3258
$\dfrac{D}{r}$	-12.1136	6.02704	15.7715	0	-31.8117	-12.3117

CHAPTER 7

CONCLUSION

Summary and Conclusion

This research takes the concepts of a coupling strength analysis from MDO and applies it to a real event that occurred on the Ares 1. An uncertainty approach is conducted to determine if there is any uncertainty while modeling the T/O event that occurred on the Ares 1. These uncertainties are within each subsystem itself as the T/O event is a turbulent event on itself cause unknown random phenomena to occur. To capture where the uncertainty realized the analysis focused to determine the coupling strength values under uncertainty. This gives a more accurate measurement of how the coupling interaction can be gaged while designing the system. Through the breakdown of the system three major disciples where analyzed in the beginning then two more disciples were found to have some impact on the T/O event. It was shown that any displacement of the length of the inhibitor has a strong effect on the T/O event based on how it effects the coupling interactions between structures and fluids. This held true with the uncertainty analysis, even though the coupling had the highest frequency of being zero the average coupling was strong and has a huge impact on the T/O event therefore effecting the value. This research paper is an advocate of capture uncertainty with the use of coupling strength analysis to determine a more accurate result for how the couplings behave under turbulent phenomena.

To understand how the uncertainty of each coupling strength measurement effected the overall value of the system a value function was developed from the field of VBD. This value function is a combination of both the Ares 1 and Congressional value functions. The

value function presented his a flexible for multiple mission profiles and can be adapted to different mission. The analysis aids the designer in make decisions based on the overall value of the system instead of it the design means the minimum specifications. By doing this the project value can be predicted and the value of the system can be used to determine the impact it has on future programs. To tie the value function with the coupling analysis a suspension of each coupling was made to evaluate how the change in coupling measurement captured in the Monte Carlo simulation had an effect on the overall system value. It was noticed that the interactions of structures and fluids had the largest impact on the overall value even under uncertainty. It is important to capture uncertainty as it aids in understanding how the subsystems interact with each other under turbulent conditions.

REFERENCES

1. Hajela, P., Christina L. Bloebaum, and Jaroslaw Sobieszczanski-Sobieski. "Application of global sensitivity equations in multidisciplinary aircraft synthesis." Journal of Aircraft 27.12 (1990): 1002-1010.

2. Constellation program: Ares I-X flight test vehicle. Retrieved from https://www.nasa.gov/pdf/354470main_aresIX_fs_may09.pdf

3. Zhang Q, Wei Z, Su W, Li J, Wang N. Theoretical modeling and numerical study for thrust-oscillation characteristics in solid rocket motors. Journal of Propulsion and Power 2012; 28:2. p. 312-322

4. Culick FEC. Combustion instabilities in solid propellant rocket motors. Internal Aerodynamics in Solid Rocket Propulsion, Belgium. 2002.

5. Constellation. Constellation finalizes thrust oscillation fix. 21 December 2009. Retrievedfrom https://blogs.nasa.gov/Constellation/2009/12/21/post_1261434125038/

6. Oates, Gordon C. Aerothermodynamics of gas turbine and rocket propulsion. Aiaa, 1997.

7. Bloebaum, Christina L., and A. R. McGowan. "The design of large-scale complex engineered systems: present challenges and future promise." Proceedings of the 14th AIAA/ISSMO Multidisciplinary Analysis and Optimization Conference, Indianapolis, IN, Paper No. AIAA-2012-5571. 2012.

8. NASA, NASA Systems Engineering Handbook. Vol. NASA/SP-2007- 6105 Rev1. 2007, Washington, D.C.

9. Forsberg, Kevin, and Harold Mooz. "7.17. System Engineering for Faster, Cheaper, Better." INCOSE International Symposium. Vol. 8. No. 1. 1998.

10. Collopy, Paul. "Economic-based distributed optimal design." AIAA Space 2001 Conference and Exposition. 2001.

11. Castagne, Sylvie, et al. "Value driven design optimization of aircraft structures." 6th AIAA Aviation Technology, Integration and Operations Conference (ATIO). 2006.

12. Buede, D.M., The Engineering Design of Systems : Models and Methods. Vol. 55. 2009: John Wiley & Sons

13. Martins, Joaquim RRA, and Andrew B. Lambe. "Multidisciplinary design optimization: a survey of architectures." AIAA journal 51.9 (2013): 2049-2075.

14. English KW. Development of multiple cycle coupling suspension in multidisciplinary design optimization. M.S Thesis. State University of New York at Buffalo 1998.

15. Sobieszczanski-Sobieski, Jaroslaw. "A linear decomposition method for large optimization problems. Blueprint for development." (1982).

16. Bloebaum, Christina L., Prabhat Hajela, and Jaroslaw Sobieszczanski-Sobieski. "Non-hierarchic system decomposition in structural optimization." Engineering Optimization+ A35 19.3 (1992): 171-186.

17. Sobieszczanski-Sobieski, J., Sensitivity of complex, internally coupled systems. AIAA journal, 1990. 28(1): p. 153-160.

18. Browning, Tyson R. "Applying the design structure matrix to system decomposition and integration problems: a review and new directions." IEEE Transactions on Engineering management 48.3 (2001): 292-306

19. Bloebaum, C., and J. Sobieszczanski-Sobieski. "Sensitivity based coupling strengths in complex engineering systems." 34th Structures, Structural Dynamics and Materials Conference. 1993.

20. Souto, Carlos d'Andrade. "Liquid rocket combustion chamber acoustic characterization." Journal of Aerospace Technology and Management 2.3 (2010): 269-278.

21. Yang, Vigor, Joseph M. Wicker, and Myong W. Yoon. "Acoustic waves in combustion chambers." Liquid rocket engine combustion instability(A 96-11301 01-20), Washington, DC, American Institute of Aeronautics and Astronautics, Inc.(Progress in Astronautics and Aeronautics. 169 (1995): 357-376.

22. Laudien, E., et al. "Experimental procedures aiding the design of acoustic cavities." Progress in Astronautics and Aeronautics 169 (1995): 377-402.

23. Young, H.D.; and Freedman, R.A.; Ford, A.L. (contributing author). 2012. Sears and Zemansky's University Physics with Modern Physics. 13th ed.Pearson Education, Inc., Addison-Wesley, San Francisco, CA, USA

24. D. J. Inman. "Engineering Vibration", 3rd Edition. Upper Saddle River, NJ, 2008, Pearson Education, IncThrust

25. Culick, F. E. C., and K. Magiawala. "Excitation of acoustic modes in a chamber by vortex shedding." Journal of Sound and Vibration 64.3 (1979): 455-457.

26. CD-adapco. STAR-CCM+ 9.06.009 [computer software]. New York, Melville 2014

27. Doston, KW, Koshigoe A. Vortex shedding in a large solid rocket motor without inhibitors at the segment interfaces. Journal of Propulsion and Power 1997; 13:2. p. 197-206.

28. Kenny RJ, Hulka J, Jones G. Cold flow testing for liquid propellant rocket injector scaling and throttling. 42nd AIAA/ASME/SAE/ASEE Joint Propulsion Conference, Sacramento, 2006.

29. Hunt, Julian CR, Alan A. Wray, and Parviz Moin. "Eddies, streams, and convergence zones in turbulent flows." (1988).

30. Moffatt, H. K. "Viscous and resistive eddies near a sharp corner." Journal of Fluid Mechanics 18.01 (1964): 1-18.

31. Knisely, Charles W. "Strouhal numbers of rectangular cylinders at incidence: a review and new data." Journal of Fluids and Structures 4.4 (1990): 371-393.

32. Mason, Donald, et al. "Pressure oscillations and structural vibrations in space shuttle RSRM and ETM-3 motors." 40th AIAA/ASME/SAE/ASEE Joint Propulsion Conference and Exhibit. 2004.

33. ANSYS Inc. ANSYS 15.0 [computer software] Pennsylvania, Canonsburg 2013

34. Dotson, K. W., S. Koshigoe, and K. K. Pace. "Vortex shedding in a large solid rocket motor without inhibitors at the segment interfaces." *Journal of Propulsion and Power* 13.2 (1997): 197-206.

35. Chapline, Gail. *Journal of Materials and Manufacturing*. Warrendale, PA: SAE International, 2006. Web

36. Guery, J., et al. "Thrust oscillations in solid rocket motors." *44th AIAA/ASME/SAE/ASEE Joint Propulsion Conference & Exhibit*. 2008.

37. Blomshield, Fred. "Lessons learned in solid rocket combustion instability." *43rd AIAA/ASME/SAE/ASEE Joint Propulsion Conference & Exhibit*. 2007.

38. Zill, Dennis G. *A First Course In Differential Equations.* 5th ed. Pacific Grove, Calif: Brooks/Cole, 2001. Print.

39. Ballereau, Severine, et al. "Evaluation method of thrust oscillations in large SRM-application to segmented SRM's." *47th AIAA/ASME/SAE/ASEE Joint Propulsion Conference & Exhibit*. 2011.

40. Davenas, Alain, ed. *Solid rocket propulsion technology*. Newnes, 2012.

41. Mark Wade (17 November 2011). "J-2X". Encyclopedia Astronautica.

42. Hazelrigg, George A. "A framework for decision-based engineering design." *Transactions-American Society of Mechanical Engineers Journal of Mechanical Design* 120 (1998): 653-658.

43. Boehm, Barry. "Value-based software engineering: reinventing." *ACM SIGSOFT Software Engineering Notes* 28.2 (2003): 3.

44. Boehm, Barry W. *Software engineering economics*. Vol. 197. Englewood Cliffs (NJ): Prentice-hall, 1981.

45. Mesmer, Bryan L., C. L. Bloebaum, and H. Kannan. "Incorporation of value-driven design in multidisciplinary design optimization." *10th World Congress on Structural and Multidisciplinary Optimization*. 2013.

46. Collopy, Paul D., and Peter M. Hollingsworth. "Value-driven design." *Journal of Aircraft* 48.3 (2011): 749-759.

47. Rogers, J. A. M. E. S., and Christina Bloebaum. "Ordering design tasks based on coupling strengths." *5th Symposium on Multidisciplinary Analysis and Optimization*. 1994.

48. ATK Space Systems, Janssen, J. *Pressure/Thrust Oscillation Forcing Functions for the SLS Booster*. EM001407 Rev. B.

49. ATK Space Systems, Janssen, J. *Pressure/Thrust Oscillation Transient Forcing Functions for the SLS Booster Motor*. TR027646 Rev. C.

50. ATK Space Systems, Kofford, A. Milano, D. *Ares 1 Dynamic Pressure to Force Conversion*. TR022382 Rev. A.

51. Collopy, Paul. "Aerospace system value models: A survey and observations." *AIAA Space 2009 Conference & Exposition*. 2009.

52. Sobieszczanski-Sobieski, Jaroslaw, and Raphael T. Haftka. "Multidisciplinary aerospace design optimization: survey of recent developments." *Structural optimization* 14.1 (1997): 1-23.

53. Bloebaum, C. L. "Coupling strength-based system reduction for complex engineering design." *Structural and Multidisciplinary Optimization* 10.2 (1995): 113-121.

54. BLOEBAUM, CHRISTINA. "Global sensitivity analysis in control-augmented structural synthesis." *27th Aerospace Sciences Meeting*. 1989.

55. Sobieszczanski-Sobieski, Jaroslaw, Christina L. Bloebaum, and Prabhat Hajela. "Sensitivity of control-augmented structure obtained by a system decomposition method." *AIAA journal* 29.2 (1991): 264-270.

56. Dantzig BG. Linear programming under uncertainty. Management Science 1955; 1(3-4): 197-206.

57. Freund RJ. The introduction of risk into a programming model. Econometrica 1956; 24(3): 253-263.

58. Zang TA, Hemsch MJ, Hilburger MW, Kenny SP, Luckring JM, Maghami P, Padula SL, Stroud WJ. Needs and opportunities for uncertainty-based multidisciplinary design methods for aerospace vehicle. NASA/TM-2002-211462, Langley Research Center, 2002

59. DeLaurentis DA, Mavris DN. Uncertainty modeling and management in multidisciplinary analysis and synthesis. In: 38th aerospace sciences meeting and exhibit, Reno, NV, AIAA-2000-0422, 2000

60. Dantzig BG. Linear programming under uncertainty. Management Science 1955; 1(3-4): 197-206.

61. Subrin, Robert. The cass for Mars. Simon and Schuster, 2012

62. Follett, Andrew. "The Wrong Right Stuff: Why NASA Consistently Fails at Congress." (2013).